# NUMERICAL INVESTIGATION OF LAMINAR MIXED CONVECTION IN TROMBE WALL CHANNEL

Asst. Prof. Dr. Saad M. Saleh
Mech. Engr. Dept .
College of Engineering
University of Baghdad

Yasser A. Abd
Mechanical Engineer

**ABSTRACT**

The two dimensional steady, combined forced and natural convection in vertical channel is investigated for laminar regime. To simulate the Trombe wall channel geometry properly, horizontal inlet and exit segments have been added to the vertical channel. The vertical walls of the channel are maintained at constant but different temperature while horizontal walls are insulated. A finite difference method using up-wind differencing for the nonlinear convective terms, and central differencing for the second order derivatives, is employed to solve the governing differential equations for the mass, momentum, and energy balances. The solution is obtained for stream function, vorticity and temperature as dependent variables by iterative technique known as successive substitution with overrelaxation. The flow and temperature patterns in the channel are obtained for Reynolds numbers and Grashof number ranging from 25 to 100 and (100 to 1,000,00,) respectively.

A computer program ( **Fortran 90** ) is built to calculate the fraction factor and the total average Nusselt number (*Nu*) also the average heat transfer *Q* in steady state and for Aspect ratio Ar (10) and Grashof number GR ($10^2 - 10^5$), the fluid Prandtl number is fixed at (Pr=0.733) and Reynolds number *Re* (25-100).

The results show reasonable representation to the relation between Nusselt number and friction factor with other parameters (Ar, GR and *Re*). *Nu* is increased with increasing Re and GR but it decreases with Ar increase and (*Q*) is increased with increasing Re ,GR and Ar. At the same time, the product friction factor(*fRe*) increased with (GR) and (Ar)increased and (*Re* )decrease.

Comparison of the result with the previous work shows a good agreement.

**الخلاصة**

**دراسة الحمل الحراري ثنائي الأبعاد المنتظم والمختلط القسري والطبيعي في قناة عمودية بالنسبة للنظام الطباقي. ومن اجل دراسة هندسة قناة تروب الجدارية بصورة صحيحة، تمت اضافة قطع إدخال وإخراج أفقية الى القناة العمودية. وتم حفظ الجدران العمودية بدرجات حرارية ثابتة ولكن مختلفة بينما تم عزل الجدران الأفقية. وقد استخدم طريقة الفروق المحددة بأستخدام طريقة الفرق ( up-wind) للحدود الحمل الحرارية اللاخطية وطريقة الفرق المركزي للمشتقات من الدرجة الثانية من اجل حل المعادلات التفاضلية الحاكمة والموزونة هي الكتلة والزخم والطاقة. والحصول على حل لدالة الأنسياب والدوامية ودرجة الحرارة كمتغيرات معتمدة بواسطة التقنية التكرارية كبديل تتابعي ذي ارتخاء زائد. وقد تم الحصول على نماذج جريان ودرجة الحرارة في القناة لأرقام رينولدز وكراشوف التي تتراوح مابين 25 الى 100 و 100 الى 1000000 على التوالي.**

تم بناء برنامج حاسوبي من نوع( فورتران 90) لحساب معامل الاحتكاك *fRe* و رقم نسلت*Nu* , ومعدل انتقال الحرارة *Q* في الحالة المستقرة وكذلك للنسبة الباعية (10) ورقم كراشوف (100-100000) ورقم براندتل تم تثبيته على (733,. ) ورقم رينولدز (25-100).
وأظهرت النتائج تميثيلا" للعلاقة مابين معدل رقم نسلت ومعدل الحرارة ومعامل الاحتكاك مع بقية المعاملات بواسطة رسم مخططات تمثل تأثير كل من (*Re*, GR ,Ar) على قيمة *Nu* , *Q* و *fRe* . وبصورة عامة، فأن رقم نسلت سوف يزداد مع زيادة كلا" من *Re* و GR ولكنه يقل بزيادة Ar أما معدل الحرارة يزداد بزيادة *Re* , GR و Ar وفي نفس الوقت، فأن معامل الاحتكاك سوف يزداد مع زيادة (GR, Ar) وانخفاض *Re*.

**KEY WORDS: Flow and Heat Transfer, Laminar, Mixed Convection, Trombe Wall Channel.**

## INTRODUCTION

The class of internal natural and mixed convection problems has significant potential for application to thermosyphon technology, heat transfer in air gaps in building walls, and nuclear reactors. Rapidly growing acceptance of solar energy as the means of heating and cooling has further stimulated research in the area of thermo-gravitational flows in open - ended cavities and parallel wall channel configuration that simulate passive solar systems such as the Trombe wall.

In a typical Trombe wall configuration, the solar energy is absorbed in the black - painted, south - facing storage wall. The resultant high temperature of the wall face drives the flow through the narrow gap. This chimney effect causes the cooler air from a room to be drawn in the from the bottom vent in the wall. This is usually referred to as the natural convection mode. Two addition modes, namely, forced and combined forced and natural modes, are possible when a mechanical device such as a blower is used to circulate the air for achieving better control of heat transport. The incident energy is also transferred to the conditioned space by conduction through the storage wall. The fluid mechanical and thermal analyses of a Trombe wall system are complicated due to several factors. It has been reported by **(Robert, 1978)** that the flow in the channel, in either free or forced modes, can be laminar or turbulent depending on the applied temperature difference ( Grashof number dependent effect in the natural convection mode), velocity (Reynolds number dependent effect in the forced mode), and the geometrical parameters characterizing the Trombe wall channel geometry. The sharp convex corners and the attend adverse local pressure gradients can also cause the flow to separate and for large recirculating eddies in the channel. In view of the complexities of the problem, a prudent approach would rule out the consideration of the problem in its entirety. Such an attempt would also obscure

the effects of individual factors on the internal natural convection phenomenon. in the present work, only the

fluid mechanical and heat transfer characteristics of combined forced and natural convective modes in laminar regime are investigated. And the present work investigates numerically the flow and heat transfer characteristics of a Trombe wall-like channel operating in the mixed convection mode with constant wall temperature condition by solving full elliptic Navier-stokes and energy equations. Also expose the ability reach the best theoretical design for Trombe wall channel for more powerful thermal energy stored through day and use it in heating of the buildings.

**GOVERNING EQUATIONS**

Steady state, two dimensional , incompressible, fully developing laminar flow

Accordingly the governing, continuity, momentum and energy conservation as follows **(Nogotov, 1978)**:-

Continuity equation:

$$\frac{\partial u}{\partial x}+\frac{\partial v}{\partial y}=0 \qquad (1)$$

Momentum Equation:

$$\frac{\partial u}{\partial t}+u\frac{\partial u}{\partial x}+v\frac{\partial u}{\partial y}= -\frac{1}{\rho}\frac{\partial p}{\partial x}+\nu\left[\frac{\partial^2 u}{\partial x^2}+\frac{\partial^2 u}{\partial y^2}\right] \qquad (2)$$

$$\frac{\partial v}{\partial t}+u\frac{\partial v}{\partial x}+v\frac{\partial v}{\partial y}= -\frac{1}{\rho}\frac{\partial p}{\partial y}+\nu\left[\frac{\partial^2 v}{\partial x^2}+\frac{\partial^2 v}{\partial y^2}\right]+g\beta\Delta T \qquad (3)$$

Energy Equation:

$$\frac{\partial T}{\partial t}+u\frac{\partial T}{\partial x}+v\frac{\partial T}{\partial y} =\alpha\left[\frac{\partial^2 T}{\partial^2 x}+\frac{\partial^2 T}{\partial y^2}\right] \qquad (4)$$

The dimensionless form:

($X= x/b$) (6)

($Y= y/b$) (5)

( $U = u/v_\infty$ ) (6)

( $V = v/v_\infty$ ) (7)

$P = p/\rho v_\infty^2$ (8)

$$\theta=\frac{T-T_\infty}{T_w-T_\infty} \qquad (9)$$

$$Gr=\frac{g\beta\Delta T\, b^3}{\nu^2} \qquad (10)$$

$\tau = t\, v_\infty / b$ (11)

$Pr = \alpha/ \nu$ (12)

$Re = v_\infty b/\nu$ (13)

By using these dimensionless forms, can be written the equations of continuity, momentum and energy as follows.

$$\frac{\partial U}{\partial X}+\frac{\partial V}{\partial Y}=0 \qquad (14)$$

$$\frac{\partial U}{\partial \tau}+U\frac{\partial U}{\partial X}+V\frac{\partial U}{\partial Y}= -\frac{\partial P}{\partial X}+\frac{1}{\mathrm{Re}}\left[\frac{\partial^2 U}{\partial X^2}+\frac{\partial^2 U}{\partial Y^2}\right] \qquad (15)$$

$$\frac{\partial V}{\partial \tau}+U\frac{\partial V}{\partial X}+V\frac{\partial V}{\partial Y}= -\frac{\partial P}{\partial Y}+\frac{1}{\mathrm{Re}}\left[\frac{\partial^2 V}{\partial X^2}+\frac{\partial^2 V}{\partial Y^2}\right]+\frac{Gr}{\mathrm{Re}^2}\theta$$

(16)

$$\frac{\partial\theta}{\partial\tau}+U\frac{\partial\theta}{\partial X}+V\frac{\partial\theta}{\partial Y}= \frac{1}{\mathrm{Pr}\,\mathrm{Re}}\left[\frac{\partial^2\theta}{\partial X^2}+\frac{\partial^2\theta}{\partial Y^2}\right] \quad (17)$$

The equations (14, 15, 16 and 17) are depend on the variable (U,V,P,θ) which are called the dependent variable. Combining the definition of vorticity and the velocity components in the terms of vorticity, and cross-differentiating the equations to reduce the number of equations and eliminate the pressure terms, a new vorticity transport equation is obtained **(Samarsky, 1971):**

$$\frac{\partial\omega}{\partial\tau}+\frac{\partial(U\omega)}{\partial X}+\frac{\partial(V\omega)}{\partial Y} =\frac{Gr_b}{\mathrm{Re}^2}\frac{\partial\theta}{\partial X}+\frac{1}{\mathrm{Re}}\left[\frac{\partial^2\omega}{\partial X^2}+\frac{\partial^2\omega}{\partial Y^2}\right] \quad (18)$$

For this flow field, the only non-zero component of the vorticity is:

$$\omega=\frac{\partial V}{\partial X}-\frac{\partial U}{\partial Y} \quad (19)$$

From the definition of stream function which verify the continuity equation, vertical and horizontal velocity components can be written as:-

$$V=-\frac{\partial\psi}{\partial X} \quad (20)$$

$$U=\frac{\partial\psi}{\partial Y} \quad (21)$$

By substituting equation (20) and equation (21) in to the equation (19) to obtain the following stream equation:

$$-\omega=\frac{\partial^2\psi}{\partial X^2}+\frac{\partial^2\psi}{\partial Y^2}=\Delta^2\psi \quad (22)$$

Energy equation become:

$$\frac{\partial\theta}{\partial\tau}+\frac{\partial(U\theta)}{\partial X}+\frac{\partial(V\theta)}{\partial Y} =\frac{1}{\mathrm{Pr}\mathrm{Re}}\left[\frac{\partial^2\theta}{\partial X^2}+\frac{\partial^2\theta}{\partial Y^2}\right] \quad (23)$$

Initial Conditions;

Initial conditions may be chosen as zero:

$\Psi=\omega=\theta=U=V=0$ (No slip condition)

Boundary Conditions;

The imposed boundary conditions, rewritten in terms of stream function and vorticity, with reference to figure (1.1), are:

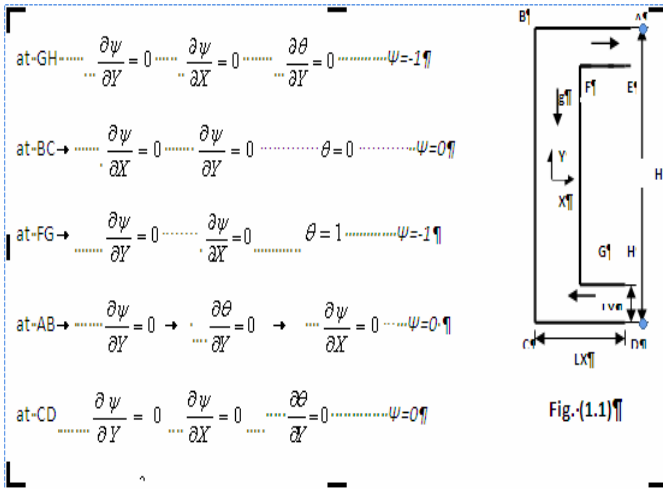

Fig.·(1.1)

**NUMERICAL SOLUTION**

By developed method for the numerical solution results by **(Samarsky, 1971)**:

$$\theta_{i,j}=\frac{a_\theta\theta_{i+1,j}+b_\theta\theta_{i-1,j}+c_\theta\theta_{i,j+1}+d_\theta\theta_{i,j-1}}{A_\theta} \quad (24)$$

Where

$$a_\theta=[(1+0.5|U_{i+1/2,j}|\,\mathrm{Pr}\,\mathrm{Re}h)\,\mathrm{Pr}\,\mathrm{Re}h]^{-1} -0.5(\,U_{i+1/2,j}-|U_{i+1/2,j}|\,) \quad (25)$$

$$b_\theta=[(1+0.5|U_{i-1/2,j}|\,\mathrm{Pr}\,\mathrm{Re}\,h)\,\mathrm{Pr}\,\mathrm{Re}\,h]^{-1} +0.5(\,U_{i-1/2,j}-|U_{i-1/2,j}|\,) \quad (26)$$

$$c_\theta=[(1+0.5|V_{i,j+1/2}|\,\mathrm{Pr}\,\mathrm{Re}h)\,\mathrm{Pr}\,\mathrm{Re}h]^{-1} -0.5(\,V_{i,j+1/2}-|V_{i,j+1/2}|\,) \quad (27)$$

$$d_\theta=[(1+0.5|V_{i,j-1/2}|\,\mathrm{Pr}\,\mathrm{Re}h)\,\mathrm{Pr}\,\mathrm{Re}h]^{-1} +0.5(\,V_{i,j-1/2}-|V_{i,j-1/2}|\,) \quad (28)$$

$$A_\theta=a_\theta+b_\theta+c_\theta+d_\theta \quad (29)$$

$$\omega_{i,j}=\frac{a_\omega\omega_{i+1,j}+b_\omega\omega_{i-1,j}+c_\omega\omega_{i,j+1}+d_\omega\omega_{i,j-1}}{A_\omega} +\frac{(Gr/2\mathrm{Re}^2)(\theta_{i+1,j}-\theta_{i-1,j})}{A_\omega} \quad (30)$$

$$\psi_{i,j}=\frac{\psi_{i+1,j}+\psi_{i-1,j}+\psi_{i,j+1}+\psi_{i,j-1}+h^2\omega_{i,j}}{4} \quad (31)$$

Where

$$a_\omega=[(1+0.5|U_{i+1/2,j}|\,\mathrm{Re}\,h)\,\mathrm{Re}\,h]^{-1} -0.5(\,U_{i+1/2,j}-|U_{i+1/2,j}|\,) \quad (32)$$

$$b_\omega=[(1+0.5|U_{i-1/2,j}|\,\mathrm{Re}\,h)\,\mathrm{Re}\,h]^{-1} +0.5(\,U_{i-1/2,j}-|U_{i-1/2,j}|\,) \quad (33)$$

$$c_\omega=[(1+0.5|V_{i,j+1/2}|\,\mathrm{Re}\,h)\,\mathrm{Re}\,h]^{-1} -0.5(\,V_{i,j+1/2}-|V_{i,j+1/2}|\,) \quad (34)$$

$$d_\omega=[(1+0.5|V_{i,j-1/2}|\,\mathrm{Re}\,h)\,\mathrm{Re}\,h]^{-1} +0.5(\,V_{i,j-1/2}-|V_{i,j-1/2}|\,) \quad (35)$$

$$A_\omega=a_\omega+b_\omega+c_\omega+d_\omega \quad (36)$$

The iteration procedure for $\theta_{i,j}$, $\omega_{i,j}$, and $\psi_{i,j}$ is as follows:

$$\omega_{i,j}=\frac{a_\omega\omega_{i+1,j}+b_\omega\omega_{i-1,j}+c_\omega\omega_{i,j+1}+d_\omega\omega_{i,j-1}}{A_\omega}$$

$$\theta_{i,j}^{s+1}=(1-F_\theta)\theta_{i,j}^{s} +\frac{F_\theta}{A_\theta}\left[a_\theta\theta_{i+1,j}^{s}+b_\theta\theta_{i-1,j}^{s+1}+c_\theta\theta_{i,j+1}^{s}+d_\theta\theta_{i,j-1}^{s+1}\right] \quad (37)$$

$$+\frac{(Gr/2\mathrm{Re}^2)(\theta_{i+1,j}-\theta_{i-1,j})}{A_\omega} \quad (38)$$

$$\psi_{i,j}^{s+1}=(1-F_\psi)\psi_{i,j}^{s} +\frac{F_\psi}{A_\psi}\begin{bmatrix}a_\psi\psi_{i+1,j}^{s}+b_\psi\psi_{i-1,j}^{s+1}\\+c_\psi\psi_{i,j+1}^{s}\\+d_\psi\psi_{i,j-1}^{s+1}+h^2\omega_{i,j-1}^{s+1}\end{bmatrix} \quad (39)$$

For all cases in the present study, an overrelaxation parameters $F_\theta, F_\psi$, and $F_\omega$ equal to 0.7, 0.5, and 0.7, are used experiments **(Gosman,1969)**.

An average vertical velocity can be calculated:

$$\overline{V} = 1/A \int_A v\, dA \qquad (40)$$

The local Nusselt number at the heated wall:

$$Nu_{L(j)} = \frac{\partial \theta}{\partial X} \qquad (41)$$

The average Nusselt number along a single channel wall is defined by **(Shih, 1984)**:

$$Nu = -\frac{1}{Ar}\int_0^{Ar}\left(\frac{\partial \theta}{\partial X}\right)_j dY \qquad (42)$$

The overall heat transfer can be calculated by:

$$Q = Ar\, Nu \qquad (43)$$

The friction factor can be obtained as follow :

$$\tau_s = \mu\, \partial v/\partial y \qquad (44)$$

The shear stress at the wall may be expressed in term of friction factor *f* as follow:

$$f(\rho \overline{V}^2/2) = \mu\, \partial v/\partial y \qquad (45)$$

By using the dimensionless parameters the equation above becomes:

$$f\,\mathrm{Re}_L = \frac{2}{\overline{V}^2}\frac{\partial V}{\partial Y} \qquad (46)$$

average *fRe* can be calculated from the equations below:

$$f\,\mathrm{Re} = \frac{1}{Ar}\int_0^{Ar} f\,\mathrm{Re}_L dY \qquad (47)$$

**DISCUSION RESULTS AND**

**Fig.1** shows indicate effects of variation of *Re* on the temperature contour maps of air. For Grashof number of $10^5$, and aspect ratio equal 10, and the inlet temperature is($\vartheta$) 0.3. Temperature contour lines are always perpendicular to the horizontal walls since an insulated boundary condition is imposed there. At low Reynolds number, the isotherms near the heated wall are found to be inclined towards the cooler left wall. As *Re* is increased, the inclination shifts towards the heated wall. This illustrates the tendency of inertial force to dominate the buoyancy force as the fluid inlet velocity increases. Also, it is noted that at low Reynolds number, there is some upstream influences indicated by the cooling of fluid in the horizontal channel even before it enters the vertical channel. As *Re* increases, this upstream influence in the lower horizontal portion of the channel decays since convection dominates the thermal diffusion of heat in the upstream direction. The temperature contour maps for low *Re* are qualitatively similar in natural

to the contour maps of free convection heat transfer in the closed vertical channel**(Yasser,2008)**.

**Fig.2** shows the effect of variation of Reynolds number on the streamline for fixed GR, aspect ratio, and inlet temperature of $10^5$, 10 and 0.3, respectively. The channel Reynolds number varied from 25 to 100. For the low Reynolds number, which the effect of free convection prevails over the effect of forced convection, the streamline pattern appears more like the one encountered in pure natural convection in a closed rectangular cavity **(Davis, 1983)**. This is clearly illustrated by the closed eddies circulating in the vertical portion of the channel. The fluid flows up in the vicinity of the hot surface and flows down on the cooler side. It is important to note that, due to stong buoyancy effects at the inner wall, there is no flow separation at the lower inner corner. Forced convection effects increase with increasing Reynolds number, and the recirculating flow patterns in the middle of the channel gradually disappears. As the Reynolds number is further increased, the closed eddies are finally " swept away " by the rapidly moving stream. Furthermore, due to increased inertia effect, the flow in the lower horizontal channel is unable to negotiate the bend, and it separates at the lower inner corner forming a separation bubble on the hot vertical surface. It is also noted that a dividing streamline ($\psi=0$) exists in the vertical channel which divides the recirculating region from the forced flow coming from the inlet.

**Fig.3** show the variation of Reynolds number on the temperature distribution of air in the channel for different GR. At constant GR, Ar=10 and *Re* equal 25and 100. for different nondimensional channel elevation of 0.2, 0.4, 0.6 and 0.8 the value of temperature dcreased with increase *Re* at fixed GR because increased the vertical velocity and the rcirculation motion decreased with increasing *Re* that lead to decrease temperature, also the temperature at elevation 0.2 is higher from inlet to mid channel because the effect of buoyancy force is higher at this part**(Yasser,2008)**.

**Fig.4** show influence variation of *Re* on the velocity profile distribution of air at nondimensional channel elevations 0.2, 0.4, 0.6 and 0.8 at constant GR. The velocity increased with increasing *Re* because increased vertical velocity and that lead to decrease the positive and negative peak velocity occurs near heated wall that result from the recirculation motion of air decreased with increased *Re* the negative peak velocity disappears dependence on the value of $Gr/\mathrm{Re}^2$.

**Fig.5** illustrates the variation of average heat transfer with *Re* through the channel for different GR ($10^2 - 10^5$). It is shown that the total heat transfer collected dependence on the Reynolds number and Grashof number. For fixed Grashof number, as Reynolds number is increased, the heat transfer from the warm wall to the fluid increases somewhat gradually while heat transfer from the circulating fluid to the cooler wall decreases sharply due to change in the flow regime. Thus, increasing the

value of *Re* implies that larger net energy is delivered to the conditioned space because of increasing the vertical velocity. Although this effect is relatively small at GR=$10^{2}$ and $10^{3}$, it is much more effect with increase value of GR at GR=$10^{4}$ and $10^{5}$ because of increasing the effect of buoyancy force and that lead to increase the intensity and the value of velocities, also the total heat transfer increased with increasing Ar because of increasing of heat transfer exchange area, the effect of GR=$10^{2}$ will be neglected**(Yasser,2008)**.

While, **Fig.6** illustrates the effect of *Re* on *fRe* value with increasing in GR. It is shown that the *fRe* decreased with increasing *Re* this effect results from increasing of vertical velocity of the flow. That lead to decrease the friction factor between the air and the wall, and the effect of GR lead to increase *fRe* with increasing GR because increased the buoyancy force (natural convection) and lead to increase the intensity and value of the vorticity of air at constant Ar **(Yasser,2008)**.

**Fig.7** show the isotherms for constant *Re*, Ar=10 and GR equal $10^{3}$ to $10^{5}$. At $10^{5}$ the isotherm patterns are qualitatively similar to those seen in Figs [(5-5c)-(5-8c)] at constant GR for different *Re* . At moderately high GR, e.g., $10^{5}$, the contour lines show nearly uniform temperature in the core region of the vertical channel and a steep temperature gradient near walls. The temperature contour maps for low *Re* and moderately high GR are also qualitatively similar to the contour maps for natural convection in the closed vertical channel. The temperature lines inclination towards hot lines increased with decrease GR until becomes uniform temperature lines**(Yasser,2008)**.

**Fig.8** show the effect of variation of GR for fixed *Re*, aspect ratio, inlet temperature of 100, 10, and 0.3, respectively and Ar=10. I note that only , the recirculating flow pattern exits in the vertical part of the at GR=$10^{5}$ channel. The recirculating due to the increased GR the effect natural convection prevails over the effect of forced convection, the stream line more likely the one encountered in pure natural convection in a closed rectangular cavity at GR=$10^{5}$, the effect is similar to keep GR fixed and reducing Reynolds number**(Yasser,2008)**.

**Fig.9** illustrate the effect of inlet temperature variation on the streamline patterns of air (Pr = 0.733) in a channel of aspect ratio (the ratio of vertical channel height, *H*, to its width, *b*). The nondimensional inlet temperature is varied from 0.0 to 1.0 while the Grashof number and Reynolds number for these cases are fixed at $10^{5}$ and 100, respectively. The scale is exaggerated in the horizontal direction to illustrate more clearly the flow features in the vertical portion of the channel. It is noted that, for most inlet temperature values, a large recirculating motion exists in the vertical channel. However, as inlet temperature decreases,

the strength as well as the extent of the recirculating motion decreases, At higher values of the temperature recirculating pattern extends to the lower horizontal part of the channel, the stream lines are qualitatively similar to those seen in **Fig.8**. At GR decrease from ($10^5$ -$10^5$) with constant *Re***(Yasser,2008)**.

**Comparison of the Results**

The comparison was made for the value of *Q* at the wall of the channel , temperature and velocity profiles at mid section across the vertical channel with the previous results obtained by **(Chaturvedi,1988)**. These comparison are shown in **Fig.10**. From these figures, a difference (approximately 13%) is found between these results.

**CONCLUSIONS**

1- The flow patterns are strongly influenced by GR, and *Re*. For a fixed GR and Pr, as Reynolds number is increased the flow pattern undergoes a change from the natural convective flow patterns, characterized by strong eddying motion in the vertical channel, to forced convective flow patterns governed by boundary layer type flow on the wall hot face. Increasing the Grashof number, for a given *Re* and Pr, enlarges and intensifies the circulatory motion in the vertical channel. At low Reynolds number (natural convection limit), the flow patterns are similar to the ones found in the natural convective flow rectangular cavities

2- The shape of isotherms are also strongly influenced by the fluid mechanical parameters GR and *Re*. At low Reynolds number, the horizontal contour lines, indicating isothermal region, are clearly indicated in the middle portion of vertical channel. At high Reynolds number, representing the forced convective limit, isotherm contour maps roughly parallel to the vertical wall are developed.

3- The investigation showed a direct dependence of velocity and temperature profile on the channel elevation and fluid mechanical parameters such as *Re* and GR. Peak velocity was found to shift toward the hot wall as the Grashof number was increased.

4- The variation of inlet temperature from 0.0 to 1.0 indicated that, the recirculating flow pattern existed for most inlet temperature for $GR/\mathrm{Re}^2 \geq 0.$

5- The net energy delivered to the conditioned space is strongly governed by *Re* and GR. At high GR, the energy convected to the conditioned space can be increased substantially if the Reynolds number is increased to its forced convective limit, also energy increased with increasing Ar. And the *fRe* increases with increasing GR and Ar but decreased with increasing *Re.*

**REFERENCES**

Robert, J. L , and Trombe, F., (1978) "Experimental study of passive Air-cooled Flat - Plate Solar Collectors: Characteristics and working Balance in the Obeillo Solar House, " Energy conservation in Heating and cooling and Ventilating Buildings, Hemisphere Publishing Corp., Washington, Vol. 2, pp. 761-782.

Nogotov, E. F., (1978) Application of Numerical Heat Transfer, Hemisphere Publishing Corp., Washington.

Samarsky, A. A. (1971) " Vvedenie *v* teoriyu raznostnkyh skhem"( "Introduction to the difference secheme theory" ) , P. 496, Moskva, Nauka.

Gosman, D., (1969) Heat and Mass Transfer in Recirculating Flows, Academic Press, New York.

Shih T. M, (1984) "Numerical Heat Transfer", McGraw-Hill, Washignton,.

Davis, G., de Vahl, (1983) "Natural Convection of Air in a Square Cavity: A Bench Mark Numerical Solution," International Journal of Numerical Methods in Fluids, Vol.3, pp. 249-264.

Chaturvedi, S. K., and Huang, G. C., (1988)"Mixed Laminar convection in Trombe Wall channels" Solar Energy, Vol. 110, pp. 31-37.

Yasser, A., Al Whabb " Numerical Investigation of Laminar Mixed Convection in Tromb Wall Channel", Department of Mechanical Engineering, University of Baghdad, M.SC., 2008.

**NOMENCLATURE**

**LATIN SYMBOLS**

| | | |
|---|---|---|
| A | Surface Area | $m^2$ |
| b | Horizontal channel Width | m |
| H | Height of channel | m |
| Ar | Aspect ratio (H/b) | - |
| K | Thermal conductivity | W/m K |
| L | Length | m |
| g | Gravity acceleration | $m/s^2$ |
| Pr | Prandtl number (Pr=ν/α) | – |
| Re | Reynolds number (Re= v b/ ν) | – |
| GR | Grashof number (Gr= $\frac{g\beta b^3(T-T_\infty)}{\nu^2}$ ) | |
| p | Air pressure | $N/m^2$ |
| P | Dimensionless air pressure | - |
| h | Heat transfer coefficient | $W/m^2.K$ |
| u, v | Velocity components in x and y direction respectively | m/s |
| U, V | Dimensionless velocity components in X and Y direction | |
| $\overline{V}$ | Average vertical velocity | m/s |
| $\overline{V}$ | Dimensionless average verical velocity– | |
| T | Temperature | K |
| i,j | X and Y direction directories | - |
| x,y | Physical coordinates of the channel | m |
| X, Y | Dimensionless physical coordinates of the channel | – |
| $\dot{m}$ | Mass flow | |
| t | Time | Sec |
| $Nu_L$ | Local Nusselt number | – |
| *Nu* | Average Nusselt number | – |
| q | Overall heat transfer | W |
| Q | Dimensionless overall heat transfer | |
| f | Friction factor( $f=\frac{2}{\overline{V}^2\,\mathrm{Re}}\frac{\partial V}{\partial n}$ ) | – |
| *fRe* | Average friction factor | – |
| $f\,\mathrm{Re}_L$ | Local friction factor | – |

**Creak Symbols**

| | | |
|---|---|---|
| μ | Viscosity | kg/m.s |
| ν | Kinematic viscosity | $m^2/s$ |
| $\beta$ | Coefficient of volume expansion | 1/K |
| α | Thermal diffusivity | $m^2/s$ |
| ρ | Air density | $kg/m^3$ |
| $\tau$ | Dimensionless time | – |
| $\vartheta$ | Dimensionless temperature | - |
| $\tau_S$ | Shear stress | $N/m^2$ |
| $\psi$ | Dimensionless stream function | – |
| $\omega$ | Vorticity | – |
| $\Delta$ | Difference between two values | – |
| $\Gamma$ | Bounding mesh | - |

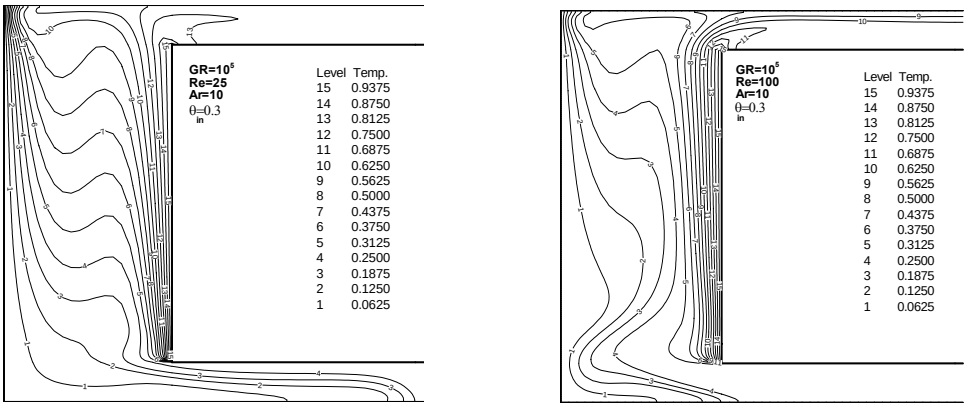


**Fig 1: Isotherm contour maps for GR=$10^5$, Ar=10 for different values of Re**

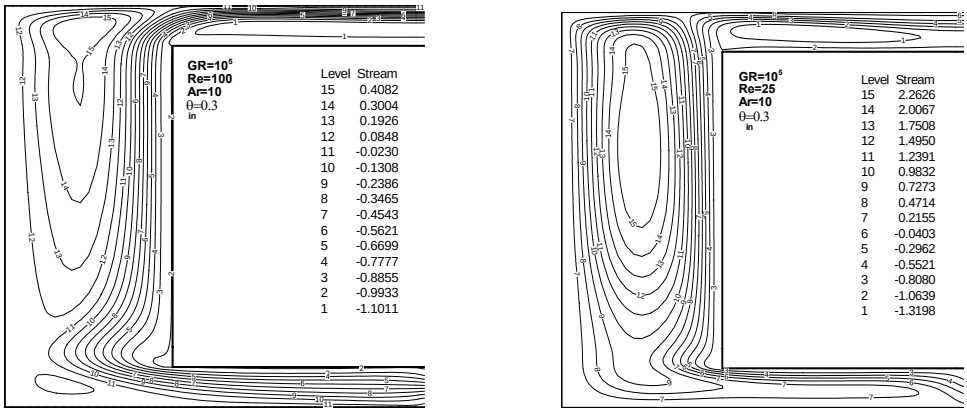


**Fig 2: Streamline contour maps for GR=$10^5$, Ar=10 for different values of Re**

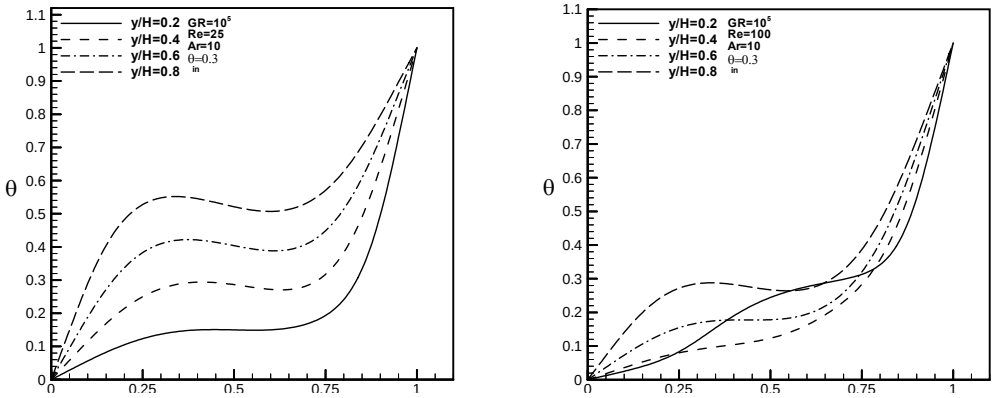


**Fig 3: Variation of temperature profile for different Reynolds number at Ar=10, GR=** $10^5$

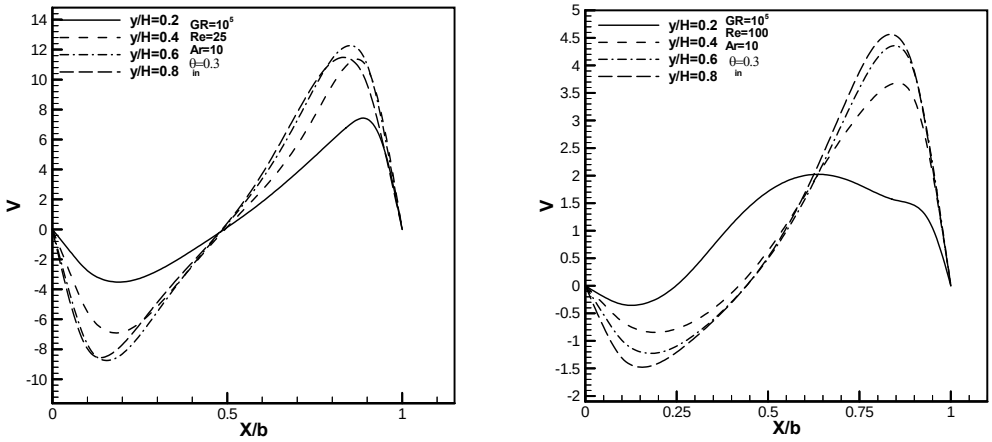


**Fig 4: Variation of velocity profile for different Reynolds number at Ar=10,**

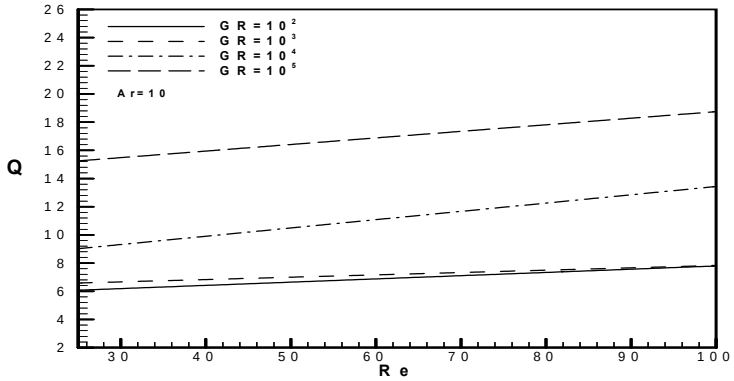


**Fig 5: Variation of *Q* with *Re* for different of GR at Ar=10**

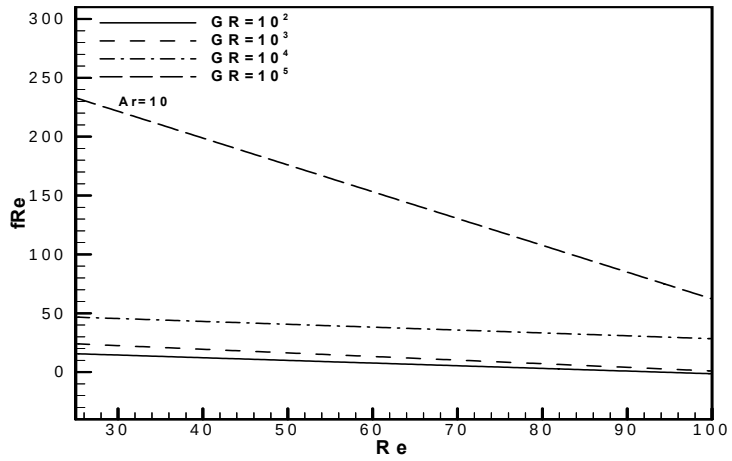


**Fig 6: Variation of *fRe* with *Re* for different values of GR**

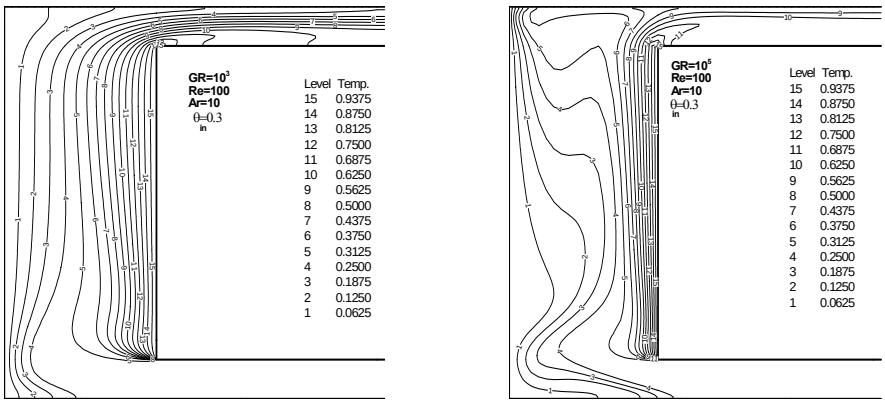


**Fig 7: Isotherm contour maps for Re=100, Ar=10 for different values of GR**

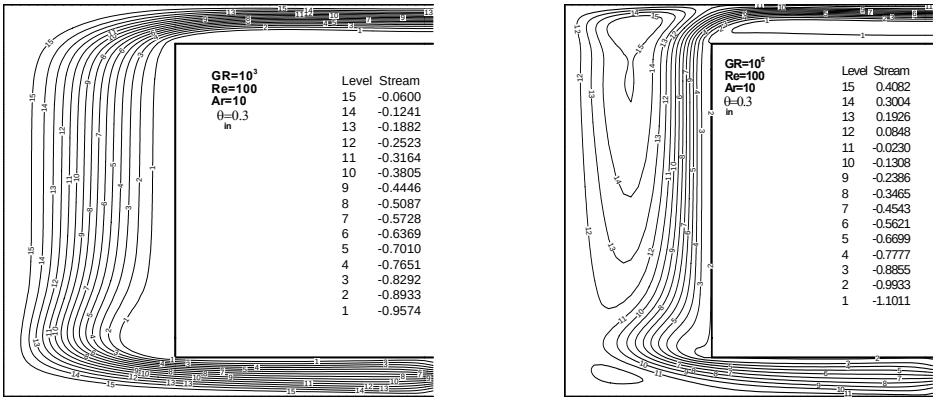


**Fig 8: Streamline contour maps for Re =100 ,Ar=10 for different values of GR**

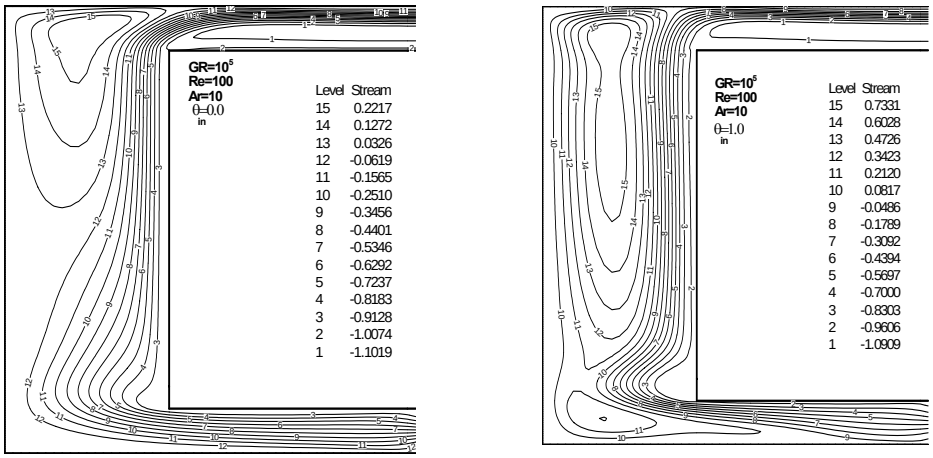


**Fig 9: Streamline contour maps for Re=100, Ar=10, *ϑ=0.0* and *1.0***

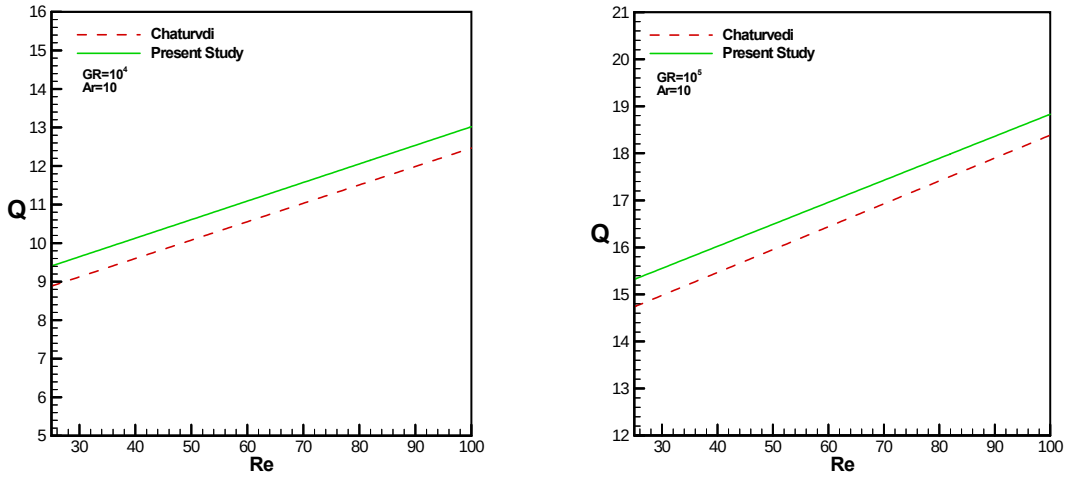


**Fig 10: Comparison between present study and (Chaturvedi, 1988) for the relation between Re and *Q* at GR=$10^4$ and GR=$10^5$**